metals

MDPI

Article

Effects of ECAP and Annealing Treatment on the Microstructure and Mechanical Properties of Mg-1Y (wt. %) Binary Alloy

Jie Wei [1,2], Guanghao Huang [1], Dongdi Yin [1,*], Kangning Li [1], Qudong Wang [2] and Hao Zhou [3]

1 Key Laboratory of Advanced Technologies of Materials, Ministry of Education, School of Materials Science and Engineering, Southwest Jiaotong University, Chengdu 610031, China; weijiesjtu@sjtu.edu.cn (J.W.); 18728435092@139.com (G.H.); 18200283550@163.com (K.L.)

2 National Engineering Research Center of Light Alloys Net Forming, School of Materials Science and Engineering, Shanghai Jiao Tong University, 800 Dongchuan Road, Shanghai 200240, China; wangqudong@sjtu.edu.cn

3 Institute of Microstructure and Property of Advanced Materials, Beijing University of Technology, Beijing 100124, China; bird0511@hotmail.com

* Correspondence: ahnydd@swjtu.edu.cn; Tel.: +86-28-8763-4673

Academic Editor: Manoj Gupta
Received: 30 December 2016; Accepted: 27 March 2017; Published: 30 March 2017

Abstract: Microstructure and mechanical properties development of extruded Mg-1Y (wt. %) binary alloy during equal channel angular pressing (ECAP) with route B_c at 400 °C, and subsequent annealing treatment between 300–400 °C at different holding time of 5–120 min were investigated using an optical and scanning electron microscope (SEM), electron back scattered diffraction (EBSD), tensile test, and hardness test. The grain size of as-extruded material (~10.9 μm) was refined significantly by 1-pass ECAP (~5.8 μm), and resulted in a remarkably enhanced elongation to failure (EL) (~+62%) with a slightly decreased ultimate tensile strength (UTS) (~−3%) comparing to the as-extruded condition (EL = 11.3%, UTS = 200 MPa). The EL was further increased to 27.3% (~+142%) after four passes of ECAP comparing to the as-extruded condition, which was mainly caused by the much more homogenized microstructure. The split basal poles with about 60° rotations to the extruded direction (ED), the relatively coarsened grain size by static recrystallization (SRX) and post-dynamic recrystallization (PDRX) after four passes of ECAP might be responsible for the decreased strength with increasing ECAP pass. During the annealing treatment, recovery dominantly occurred at 300 °C, SRX and grain growth emerged at 350 °C and 400 °C, respectively. Meanwhile, the grain grew and hardness decreased rapidly even within 5 min for 1-pass ECAPed material at 400 °C, indicating a larger grain boundary mobility of ECAPed materials induced by higher deformation energy than the as-extruded ones.

Keywords: Mg-RE alloy; equal channel angular pressing; annealing treatment; mechanical property; grain boundary mobility

1. Introduction

Nowadays, as the problems of environment and energy shortages have become more and more serious, there is a high demand for strong and lightweight materials. Magnesium (Mg) and its alloys are quite promising candidates due to their low density, high strength/weight ratio and cast capability [1]. However, the relatively low strength and ductility limit their broad applications [2].

Alloying elements, especially the rare earth (RE) elements, can remarkably improve the performance of magnesium [3,4]. Yttrium (Y), as a rare earth element, is widely introduced to magnesium alloys, which is capable of improving the performance of magnesium alloys more efficiently than aluminum, manganese [5] and some other RE elements [6,7]. Beyond that, during the deformation process, alloying yttrium can activate non-basal slip systems and improve the ductility of magnesium alloys [5,8,9].

In addition to alloying elements, processing by severe plastic deformation (SPD) is an efficiency method to improve the strength and ductility of Mg alloys [10–13]. Equal channel angular pressing (ECAP), as one of the SPD techniques, is attractive for imposing high strain to materials by multi-passes without cross-sectional dimensions changed [12,13]. The ECAP has been applied to various alloys for enhancing the mechanical properties [11,14,15]. During this process, the microstructures of ECAPed materials could be refined and homogenized by dynamic recrystallization (DRX) [16–18]. Dynamic recrystallization in magnesium and its alloys has been reported to occur by several mechanisms. According to the characteristics of the recrystallization process, these recrystallization mechanisms can be divided into two groups: continuous and discontinuous dynamic recrystallization. It is also reported that stacking fault energy, initial grain size and thermo-mechanical processing conditions could have a significant effect on DRX [19]. Moreover, DRX has been proven to influence the final microstructure and mechanical properties of the deforming specimens strongly [19–21]. In addition, there are reports that subsequent annealing treatment can release the residual stress and internal energy of ECAPed materials, resulting in a further improvement of the performance [11,22].

However, the microstructure and mechanical properties evolution of Mg-Y based alloys during ECAP, and subsequent annealing treatment are not fully understood. Recently, Zhou et al. [14] investigated the effect of ECAP on microstructure and mechanical properties of Mg-Y-RE-Zr alloy, who revealed that the first pass of ECAP process in grain refinement is more efficient than higher passes, and the intensity of (0002) basal texture increased with increasing ECAP passes. Lapovok et al. [23] reported that the annealing treatment could enhance the mechanical properties of ECAPed Mg-Y-Zn alloy, and noted that optimized properties were achieved by the ECAP process at 500 °C with subsequent annealing treatment at 400 °C for 12 min. The current paper mainly investigates the microstructure evolution and mechanical properties alteration of Mg-1Y binary alloy during ECAP and subsequent annealing treatment, focusing on the relation between microstructure and mechanical properties. The results can provide a reference for developing high-performance Mg-Y based alloys by ECAP and the related heat treatments.

2. Materials and Methods

Mg-1Y (composition in wt. %, if there is no additional statement) ingots were prepared from high purity (≥99.9%) Mg and Mg-30Y master alloys by induction melting in a mild steel crucible at approximately 750 °C under the protection of a mixed atmosphere of CO_2 and SF6 with the volume ratio of 100:1. Finally, the melts were poured into a steel mould with the diameter of 95 mm, and the ingots were homogenized at 530 °C for 8 h and cooled in air. Moreover, the actual chemical composition of the ingots was Mg-0.86Y, obtained by inductively coupled plasma spectrometer (ICP, Perkin-Elmer, Waltham, MA, USA).

The ingots were cut into a cylinder with a diameter of 90 mm from the center and extrusion was conducted at a ratio of 9:1 at 300 °C. The rectangular samples prepared for ECAP, with the geometry of 20 × 20 × 70 mm, were machined from the center of as-extruded materials. Figure 1 illustrates the procedure of ECAP, four passes with route B_c (the sample is rotated by 90° in clockwise between each pass) were performed through the H13 steel die with an internal angular (ϕ) of 90° and external angular (ψ) of 37° at 400 °C, and the stain of each pass was ~1 [12,13]. The rectangular samples were held at 400 °C for 10 min and then pressed through the die preheated to 400 °C with a press speed of ~0.6 mm·s^{-1} in each pass, with MoS_2 and graphite lubricant the channels. The average inter-pass time of each ECAP process is ~90 s. After the procedure of ECAP, the samples were quenched in water to

prevent the further growth of grain. Figure 2 shows the photographs of ECAPed samples at 400 °C for different passes, and the samples do not show any surface defects and have a similar appearance after different passes. However, there is a decreasing trend in the length of the sample with increasing passes, due to the surface sanded procedure of the samples between each pass. It is worth noting that a lower temperature pressing at 350 °C was performed, but failed to produce the sample without cracks.

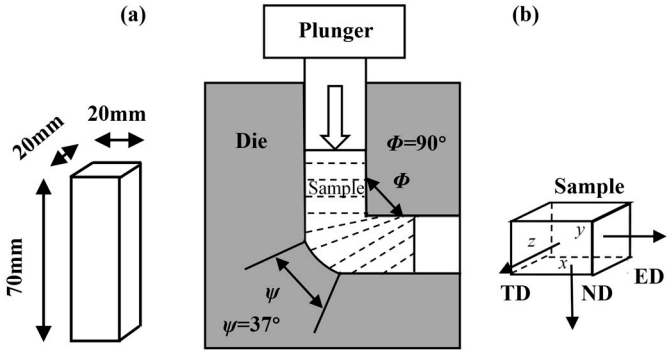

Figure 1. Schematic illustrations of (**a**) the geometry of the rectangular samples prepared for Equal channel angular pressing (ECAP); (**b**) ECAP process with reference axes. ED, TD and ND represent the extrusion direction, transverse direction and the normal direction to *x*-plane, respectively.

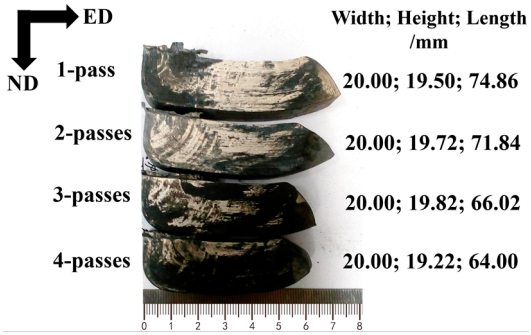

Figure 2. Photographs of ECAPed samples at 400 °C for different passes.

Annealing treatments for as-extruded and 1-pass ECAPed materials were performed at various temperatures between 300–400 °C with different holding times of 5–120 min.

The microstructural observation was conducted by using Zeiss Axio Lab A1 optical microscope (OM, Zeiss, Brno, Czech Republic) and QUANTA FEG 250 scanning electron microscope (SEM, FEI, Hillsboro, OR, USA) equipped with an Oxford Instruments-HKL channel 5 EBSD analysis system (Oxford Instruments, Abingdon, Oxfordshire, UK). For OM and EBSD, observation plane of the samples was the Extrusion Direction-Transverse Direction (ED–TD) plane, as shown in Figure 1. The grain size (d) was estimated by the linear intercept method using optical microscope images ($d = 1.74 \times L$, where L is the linear intercept grain size [24]).

The tensile properties were evaluated by a CMT-5105 universal testing machine (MTS Industrial Systems, Shenzhen, China) with a strain rate of 1×10^{-3} s^{-1} at ambient temperature. The dog bone tensile specimens, machined from the center of as-extruded and ECAPed samples, with gauge length of 8 mm and cross-sectional area of 2 × 3 mm. The longitudinal section of the specimen was parallel to the Extrusion Direction-Normal Direction (ED–ND) plane, and the tensile axis was parallel to ED (Figure 1). The tensile tests were performed at least thrice on each condition, and the averages were taken as the reported measurements. The Vickers microhardness (H_V) of the samples on the ED–TD plane were measured by HVS-30D series digital micro hardness test machine (Precision Instrument, Shanghai,

China) equipped with a diamond pyramidal indenter with an applied load of 1000 g for 10 s, at least eight separate points were randomly selected and the values of H_V were the average measurements.

3. Results and Discussion

3.1. Microstructures

Figure 3 illustrates the optical microstructures of Mg-1Y alloys with different ECAP passes. As shown in Figure 3a, after the extrusion process, plenty of coarse grains are elongated along the extrusion direction (ED), and fine grains exist around the elongated coarse grain boundaries. Stanford observed a similar phenomenon in extruded Mg-Gd alloy [25], and it is probably due to the fact that the elongated grains, which store a large amount of deformation energy, are favorable to the nucleation of recrystallization. During the pre-heat treatment before the ECAP process, the grains grow rapidly due to static recrystallization (SRX), but the distributions of the grains are much more homogenized (Figure 3b). After 1-pass, more and more coarse grains are substituted by fine grains and some fine grains coexist within the elongated coarse grains, which separate the elongated grains just like a stick bread cut by a knife. The microstructures tend to be homogenized and the grain boundaries are more distinct with passes increased. After three passes, the elongated coarse grains disappear completely, and the grains are further homogenized after four passes. However, the grain boundaries remain the serrated borders as before, which indicate that continuous dynamic recrystallization (CDRX) during the ECAP process is incomplete, and still reserve plenty of energy in the grain boundaries [26]. It is probably due to yttrium (Y) atoms segregated to the grain boundaries, which could suppress dynamic recrystallization (DRX) [21]. A larger number of grains (>1000) are measured by the linear intercept method, and the average grain size of each pass is shown in Figure 3. It needs to note that the grain size of the as-extruded sample after pre-heat treatment (~24.7 μm) was refined dramatically by the 1-pass ECAP process (~5.8 μm).

Unfortunately, the growth of grain is observed in the subsequent 1–3-passes ECAP (Figure 3). Except as mentioned above, preheating before ECAP would lead to the growth of grain, another important point should be considered: the samples are not pressed out at the same time during the ECAP process, and there would be post-DRX or SRX at 400 °C for the section which comes out earlier. This point will have pronounced impacts on the microstructure evolution and, simultaneously, mechanical properties. Bohlen et al. have proven that the extruded AZ31 samples exited from the die by air-cooling led to a change in the microstructure with coarser grains than water-cooled ones, which was related to SRX and post-DRX. Meanwhile, the air-cooled sample revealed a remarkably decreased strength compared to the water-cooled one [27]. Similar results were also observed in extruded Mg-Li-(Al) alloys [28]. Therefore, the different cooling conditions should have some influence on the development of microstructure and mechanical properties of the Mg-1Y alloy, which needs further investigation. Meanwhile, the ECAP process in the following chapters of the current paper includes pre-heat treatment and the pressed process, if there is no particular statement.

The {0001}, {11–20} and {10–10} pole figures of as-extruded and 4-pass ECAPed materials are shown in Figure 4 (the dates are from the electron back scattered diffraction measurements). In the as-extruded materials, it is evident that the {0001} basal plane shows a maximum intensity of around 5.1 MRD (multiples of random distribution) and appear to have an angle of nearly 90° with the extrusion direction (ED). Meanwhile, the {11–20} and {10–10} planes in most grains are nearly perpendicular to the normal direction (ND) with a relatively weak texture. After four passes, the {0001} basal plane presents a stronger texture with a maximum intensity of around 8.2 MRD and has an angle of about 60° with ED. It needs to be noted that a split basal texture is observed in 4-pass ECAPed materials, which might be due to the higher activity of the non-basal <c + a> slip by alloying Y [24,25] during the ECAP process.

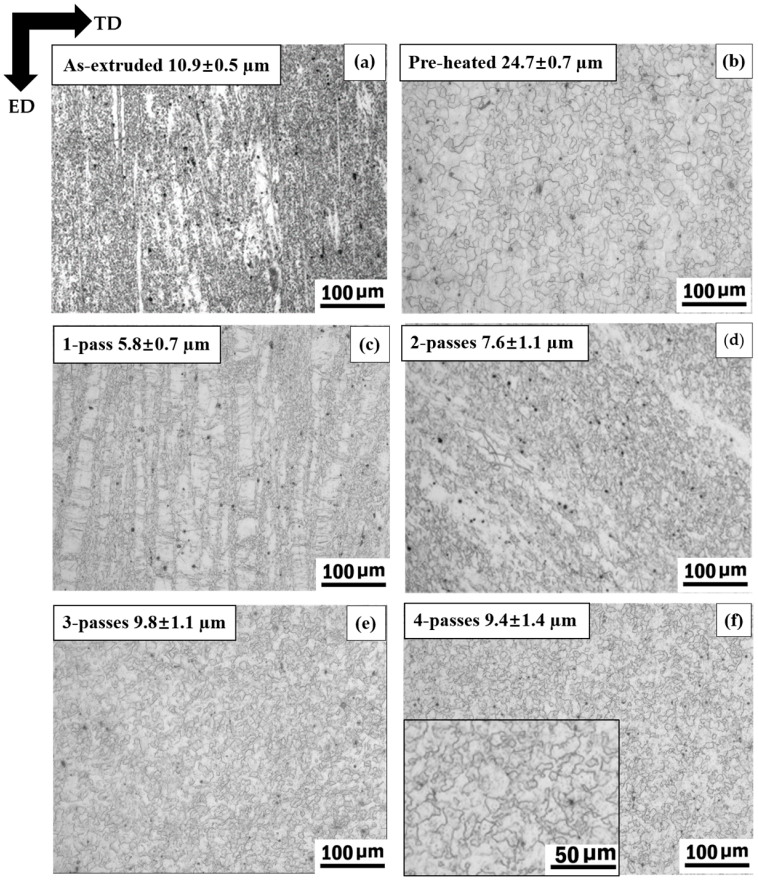

Figure 3. Optical microscope images of (**a**) as-extruded Mg-1Y alloy; (**b**) as-extruded Mg-1Y alloy treated at 400 °C for 10 min before 1-pass ECAP process; (**c**) 1-pass; (**d**) 2-pass; (**e**) 3-pass; and (**f**) 4-pass ECAPed alloys.

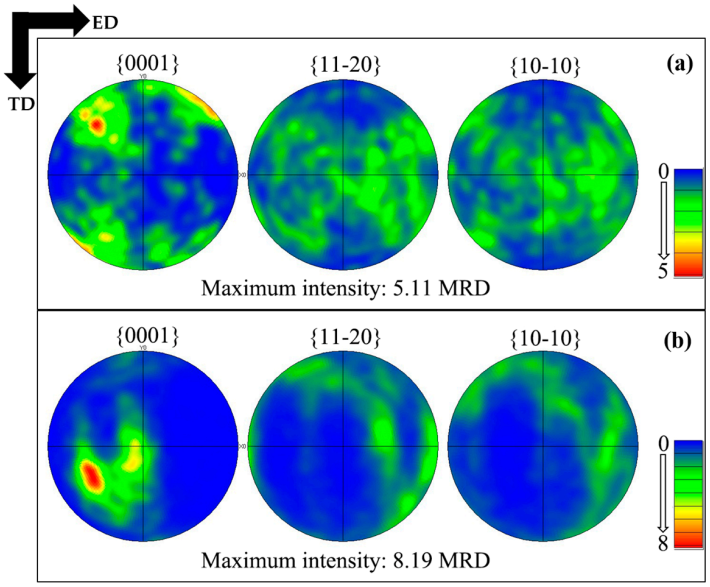

Figure 4. Pole figures of (**a**) 0-pass (as-extruded); and (**b**) 4-pass ECAP alloys (the dates are from the electron back scattered diffraction measurements).

Figure 5 illustrates the optical micrographs of as-extruded and ECAPed (1-pass) Mg-1Y after annealing at different temperatures for 60 min. The microstructures show no apparent variations at

300 °C, while, at 350–400 °C, the grain grew rapidly and the elongated coarse grains in the as-extruded and ECAPed samples disappeared due to static recrystallization (SRX). It proved that intragranular dislocation and the stored energy accumulated during deformation were released, leading to the homogenized grains. Moreover, the growth of grain with higher ECAP passes might be attributed to the rapid grain growth rate at 400 °C.

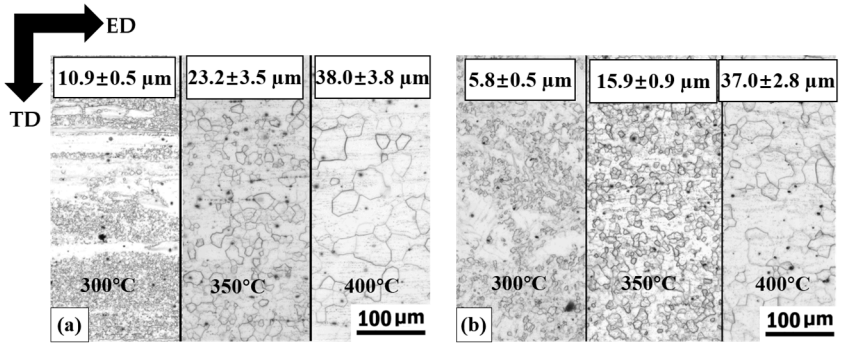

Figure 5. Optical microscope images of (**a**) as-extruded; and (**b**) ECAPed (1-pass) alloys at different annealing temperatures for 60 min.

3.2. Mechanical Properties

The tensile engineering stress–strain curves of as-extruded and ECAPed materials are presented in Figure 6. Moreover, the yield strength (YS), ultimate tensile strength (UTS) and elongation (EL) to rupture are summarized in Figure 7. The EL of Mg-1Y alloy is remarkably enhanced by 1-pass ECAP (~18.4%) compared to the as-extruded condition (~11.3%) with a slight decrease of the strength. With increasing pass, the YS and UTS decreased while the EL increased gradually. After four passes, the EL further increased to 27.3%, which is 141.6% larger than the as-extruded alloy, with 11% and 24% decrement of UTS and YS, respectively.

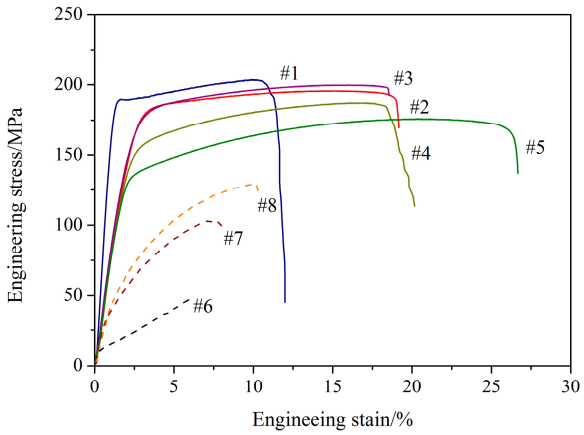

Figure 6. Tensile engineering stress–strain curves, and solid line represents current trials: (**#1**) as-extruded sample; (**#2**) 1-pass ECAPed sample; (**#3**) 2-pass ECAPed sample; (**#4**) 3-pass ECAPed sample; (**#5**) 4-pass ECAPed sample; dash line represent the trials by Ref. [29]; (**#6**) as-cast pure Mg; (**#7**) 4-pass ECAP at 360 °C (Mg); (**#8**) 1-pass ECAP at 360 °C + 3-pass ECAP at 300 °C (Mg).

Compared with the curves of as-cast pure Mg and pure Mg processed by ECAP with route A under different experimental conditions studied previously [29] (Figure 6), the mechanical behavior of pure Mg and Mg-1Y is significantly different. First, after the 4-pass ECAP process at 400 °C, YS and UTS of Mg-1Y alloy represent a decreasing trend at a similar slope, which disagrees with the

greatly increased YS and UTS of pure Mg at a lower temperature (360 °C). The main reasons are probably the increased grain size during ECAP at 400 °C and weakened basal texture by alloying yttrium. Second, after four passes, Mg-1Y alloy (YS, UTS, EL = ~132 MPa, ~178 MPa, ~27%) shows dramatically outstanding mechanical properties than pure Mg (YS, UTS, EL = ~58 MPa, ~162 MPa, ~16%), which is related to solid solution strengthening and the activation of <c + a> slip by alloying yttrium. Simultaneously, route B_c is more efficient in grain refinement than route A [12,13]. Therefore, yttrium could significantly improve the strength or enhance the ductility of Mg alloys. Furthermore, ECAP also should be able to refine grains more efficiently at a lower temperature with a premise that there are no cracks generated during the process.

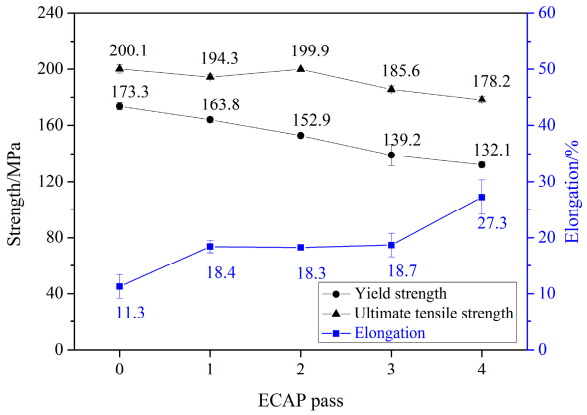

Figure 7. The mechanical properties evolution versus ECAP pass.

The curve of YS versus the square root of grain size ($d^{-1/2}$) for the alloys is shown in Figure 8. It deviated from the Hall–Petch relationship (positive slope), and the sign of yield strength versus $d^{-1/2}$ is neither positive nor negative. A similar result was found in AZ61 Mg alloys [18,24], which is due to Mg alloys having an HCP structure; therefore, texture orientation and the activation of non-basal slip can affect its mechanical properties, rather than just grain boundary strengthening (Hall–Petch relationship) [18]. According to the pole figures of as-extruded and 4-pass ECAPed materials (Figure 4), the {0001} basal plane of as-extruded rotated from about 90° to 60° with ED after the 4-pass ECAP process, which indicates that basal slip of 4-pass ECAPed material might emerge easier than the as-extruded one, due to a relatively larger Schmid factor (m).

Thus, after 1-pass ECAP process, the significant enhancement of EL (~63% larger than the as-extruded one) correlates with the remarkably refined grains. Meanwhile, the increased volumes of grain boundaries probably could not retard dislocation slide efficiently and resulted in a slightly decreased strength. After four passes, the homogenized grains play a major role in a further remarkably increased EL. Moreover, the relatively coarser grain, due to SRX during pre-heat treatment and post-DRX after the ECAP process, could also lead to the decreased strength. In addition, the texture evolution during ECAP perhaps also affects the mechanical properties, which needs further investigation.

The hardness and grain size evolution during the annealing treatment are shown in Figure 9. At 300 °C, there is a slight fluctuation of hardness with increasing annealing time. Nonetheless, the hardness decreased significantly with increasing annealing time at 350–400 °C. A higher decreased rate and lower hardness value at 400 °C compared to that at 350 °C for all the specimens tested is observed. It indicates that more dislocation and deformation energy were consumed at a higher temperature and resulted in a complete recovery. Furthermore, the grain grew rapidly at 400 °C, which might be attributed to the mobility of high angle grain boundaries (HAGs) increasing with a rise of temperature and more low angle grain boundaries (LAGs) being consumed by HAGs [30]. The grain size and hardness exhibit similar trends during annealing treatment for as-extruded and ECAPed

materials (Figure 9). However, the grain growth of the ECAPed materials is much more pronounced than as-extruded specimens at 400 °C, which is due to the samples storing more energy after ECAP than the extrusion process, resulting in a larger driving force for grain boundary immigration [30].

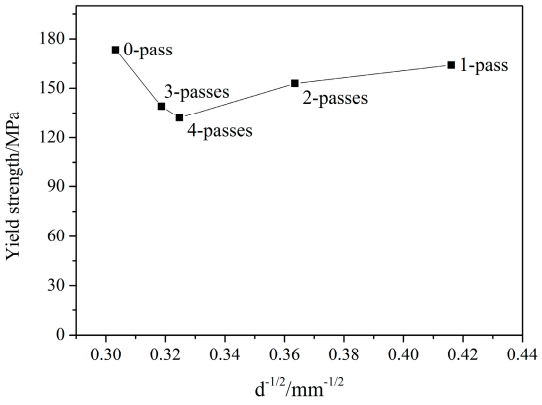

Figure 8. Yield strength versus the square root of grain size ($d^{-1/2}$) for as-extruded and ECAPed Mg-1Y alloys.

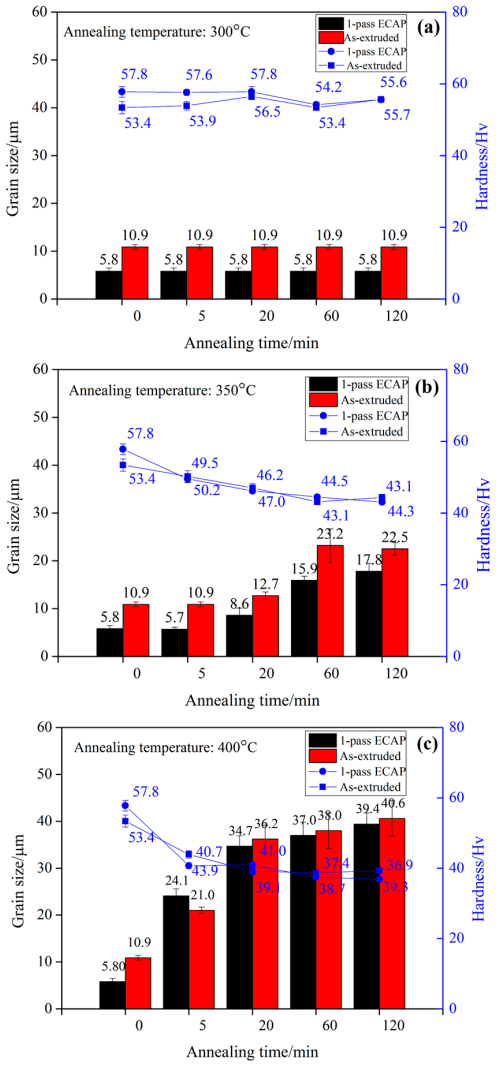

Figure 9. The grain size and hardness versus annealing time at (**a**) 300 °C; (**b**) 350 °C; (**c**) 400 °C of as-extruded, ECAPed (1-pass) materials.

During annealing treatment, recovery will emerge first and then static recrystallization (SRX) occurred. The microstructural changes in a material are subtle and occur on a small scale during recovery [30]. As aforementioned, when annealing at 300 °C, no clear variations could be observed (Figure 5). However, the hardness values versus annealing time at 300 °C show a slight fluctuation. Hence, recovery mainly occurred for Mg-1Y alloys annealing at 300 °C.

For higher temperature annealing (350–400 °C), not only recovery emerged, but static recrystallization and further grain growth also occurred. However, whether recovery or static recrystallization, the grain boundary mobility is one of the controlling factors, which can be described by the equation as follows [30]:

$$v = \left[M_0 \exp\left(-\frac{Q}{RT}\right)\right](P_d - P_{sol}), \quad (1)$$

where v is the moving velocity of grain boundary, grain boundary mobility $M = M_0 \exp\left(-\frac{Q}{RT}\right)$ is the constant during isothermal annealing, P_d is driving pressure, and P_{sol} is the retarding pressure due to solute drag. Meanwhile, the grain boundary structure, point defect and some other factors are ignored here. According to the equation, with increasing temperature, the grain boundary mobility (M) enhanced exponentially. It explains why the grain growth rate of annealing at 400 °C is much higher than that at 350 °C. Moreover, annealing treatment consistently releases deformation energy, which decreases driving force (P_d) with increasing annealing time. This therefore shows a rapid decrease rate for hardness value and grain growth when start annealing treatment. Subsequently, the rate of softening and grain growth are slowing down with increasing annealing time. Compared with Mg-6Zn-Y (at. %), whose best annealing temperature (the sample represents a refined and homogenous grain) is 400 °C [22]. However, Mg-1Y shows coarse grains and deteriorating hardness in the same conditions. The main reason is that Mg-6Zn-Y (at. %) possesses more solid atoms in grain boundaries, which slows the mobility of the grain boundary by increased P_{sol} in Equation (1). Therefore, compared to the influence of the different annealing temperatures on the microstructure and hardness, 350 °C is a suitable annealing temperature for Mg-1Y alloy.

3.3. Fractography

Figure 10 shows SEM fractography of the as-extruded and ECAPed Mg-1Y alloys. The fracture surfaces of as-extruded and ECAPed Mg-1Y are mainly composed of tear ridges, cleavage planes and dimples. With increasing ECAP passes, the proportions of cleavage planes decreased and more highly developed tearing ridges and tiny dimples were observed, which suggests that the specimen undergoes a substantial plastic deformation prior to fracture, which is consistent with the significant improvement of elongation, as aforementioned. It is worth noting that, as shown in Figure 10c, there are some tiny dimples and secondary cracks surrounding elliptic selection. Considering elongated coarse grains still existing after 2-pass ECAP and fine grains nucleated and growing around them (Figure 3d), the elliptic selection was the cleavage plane of the elongated grain.

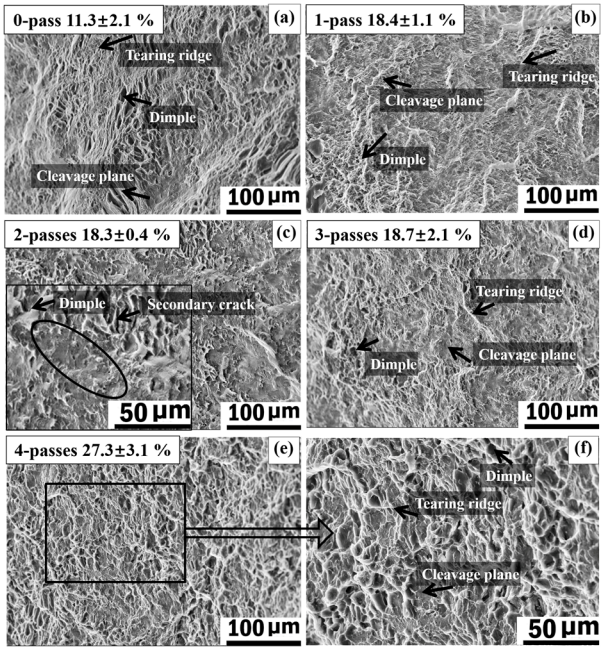

Figure 10. SEM fractography of (**a**) 0-pass (as-extruded); (**b**) 1-pass; (**c**) 2-pass; (**d**) 3-pass; (**e**) 4-pass ECAPed Mg-1Y alloys; and (**f**) higher magnification of the rectangular selection of (**e**).

4. Conclusions

The microstructure and mechanical properties of Mg-1Y alloy during ECAP with route B_c at 400 °C and subsequent annealing treatment between 300–400 °C at different holding time of 5–120 min were investigated. The main conclusions of this work are summarized as follows:

1. The grain size of as-extruded materials (~10.9 μm) is refined significantly by 1-pass ECAP (~5.8 μm), and resulted in a remarkably enhanced elongation to failure (EL) (~+62%) with a slightly decreased strength (~−3%) comparing to the as-extruded condition (EL = ~11.3%, UTS = ~200 MPa). The EL is further increased to ~27.3% (~+142%) after 4-pass ECAP compared to the as-extruded condition, which is mainly due to the much more homogenized microstructure. The split basal poles with about 60° rotations to the extruded direction (ED) and the relatively coarsened grain size by SRX and post-DRX after 4-pass ECAP might be responsible for the decreased strength with increasing ECAP pass.
2. With increasing ECAP pass, the proportions of cleavage planes decreasing and more highly developed tearing ridges, tiny dimples are observed indicating large plastic deformation occurred before fracture, which is consistent with the remarkable enhancement of the EL.
3. Annealing treatments indicate that recovery dominantly occurs at 300 °C, SRX and grain growth emerge at 350 °C and 400 °C, respectively. Meanwhile, the grain growth and hardness decrease rapidly even within 5 min for 1-pass ECAPed alloy at annealing temperature 400 °C, implying a larger grain boundary mobility induced by higher deformation energy than the as-extruded ones.

Acknowledgments: This work was supported by the National Natural Science Foundation of China (Nos. 51401172 and 51601003), the Project of Science & Technology Department of Sichuan Province (No. 2015HH0012), and Fundamental Research Funds for the Central Universities (No. 2682016CX073).

Author Contributions: Dongdi Yin and Jie Wei conceived and designed the experiments; Guanghao Huang, Jie Wei and Kangning Li performed the experiments; Jie Wei and Guanghao Huang analyzed the data; Hao Zhou contributed analysis tools; and Jie Wei, Dongdi Yin and Qudong Wang wrote the paper.

Conflicts of Interest: The authors declare no conflict of interest.

References

1. Friedrich, H.; Schumann, S. Research for a "new age of magnesium" in the automotive industry. *Mater. Process. Technol.* **2001**, *117*, 276–281. [CrossRef]
2. Avedusian, M.M.; Baker, H. *Magnesium and Magnesium Alloys, ASM Specialty Handbook*; ASM International: Materials Park, OH, USA, 1999.
3. Rokhlin, L.L. *Magnesium Alloys Containing Rare Earth Metals*; CRC Press: London, UK, 2003.
4. Tekumalla, S.; Seetharaman, S.; Almajid, A.; Gupta, M. Mechanical Properties of Magnesium-Rare Earth Alloy Systems: A Review. *Metals* **2014**, *5*, 1–39. [CrossRef]
5. Somekawa, H.; Osawa, Y.; Singh, A.; Washio, K.; Kato, A.; Mukai, T. Effect of Micro-Alloying Elements on Deformation Behavior in Mg–Y Binary Alloys. *Mater. Trans.* **2014**, *55*, 182–187. [CrossRef]
6. Gao, L.; Chen, R.S.; Han, E.H. Effects of rare-earth elements Gd and Y on the solid solution strengthening of Mg alloys. *J. Alloy Compd.* **2009**, *481*, 379–384. [CrossRef]
7. Hantzsche, K.; Bohlen, J.; Wendt, J.; Kainer, K.U.; Yi, S.B.; Letzig, D. Effect of rare earth additions on microstructure and texture development of magnesium alloy sheets. *Scr. Mater.* **2010**, *63*, 725–730. [CrossRef]
8. Suzuki, M.; Sato, H.; Maruyama, K.; Oikawa, H. Creep behavior and deformation microstructures of Mg–Y alloys at 550 K. *Mater. Sci. Eng. A* **1998**, *252*, 248–255. [CrossRef]
9. Sandlöbes, S.; Zaefferer, S.; Schestakow, I.; Yi, S.; Gonzalez-Martinez, R. On the role of non-basal deformation mechanisms for the ductility of Mg and Mg–Y alloys. *Acta Mater.* **2011**, *59*, 429–439. [CrossRef]
10. Valiev, R.Z.; Korznikov, A.V.; Mulyukov, R.R. Structure and properties of ultrafine-grained materials produced by severe plastic deformation. *Mater. Sci. Eng. A* **1993**, *168*, 141–148. [CrossRef]
11. Zhao, Y.H.; Liao, X.Z.; Jin, Z.; Valiev, R.Z.; Zhu, Y.T. Microstructures and mechanical properties of ultrafine grained 7075 Al alloy processed by ECAP and their evolutions during annealing. *Acta Mater.* **2004**, *52*, 4589–4599. [CrossRef]
12. Langdon, T.G. The principles of grain refinement in equal-channel angular pressing. *Mater. Sci. Eng. A* **2007**, *462*, 3–11. [CrossRef]
13. Valiev, R.Z.; Langdon, T.G. Principles of equal-channel angular pressing as a processing tool for grain refinement. *Prog. Mater. Sci.* **2006**, *51*, 881–981. [CrossRef]
14. Zhou, L.; Liu, Y.; Zhang, J.; Kang, Z. Microstructure and mechanical properties of equal channel angular pressed Mg–Y–RE–Zr alloy. *Mater. Sci. Technol.* **2016**, *32*, 969–975. [CrossRef]
15. Alizadeh, R.; Mahmudi, R.; Ngan, A.H.W.; Pereira, P.H.R.; Huang, Y.; Langdon, T.G. Microstructure, Texture, and Superplasticity of a Fine-Grained Mg-Gd-Zr Alloy Processed by Equal-Channel Angular Pressing. *Metall. Mater. Trans. A* **2016**, *47*, 6056–6069. [CrossRef]
16. Yamashita, A.; Horita, Z.; Langdon, T.G. Improving the mechanical properties of magnesium and a magnesium alloy through severe plastic deformation. *Mater. Sci. Eng. A* **2001**, *300*, 142–147. [CrossRef]
17. Agnew, S.R.; Horton, J.A.; Lillo, T.M.; Brown, D.W. Enhanced ductility in strongly textured magnesium produced by equal channel angular processing. *Scr. Mater.* **2004**, *50*, 377–381. [CrossRef]
18. Kim, W.J.; An, C.W.; Kim, Y.S.; Hong, S.I. Mechanical properties and microstructures of an AZ61 Mg Alloy produced by equal channel angular pressing. *Scr. Mater.* **2002**, *47*, 39–44. [CrossRef]
19. Huang, K.; Logé, R.E. A review of dynamic recrystallization phenomena in metallic materials. *Mater. Des.* **2016**, *111*, 548–574. [CrossRef]
20. Knauer, E.; Freudenberger, J.; Marr, T.; Kauffmann, A.; Schultz, L. Grain Refinement and Deformation Mechanisms in Room Temperature Severe Plastic Deformed Mg-AZ31. *Metals* **2013**, *3*, 283–297. [CrossRef]
21. Cottam, R.; Robson, J.; Lorimer, G.; Davis, B. Dynamic recrystallization of Mg and Mg–Y alloys: Crystallographic texture development. *Mater. Sci. Eng. A* **2008**, *485*, 375–382. [CrossRef]
22. Wang, L.; Min, G.H.; Gao, P.P.; Wang, X.Y.; Yu, H.S.; Cui, H.W. Effects of Annealing Treatment on the Microstructure and Mechanical Properties of Magnesium Alloy Sheets. *Appl. Mech. Mater.* **2013**, *303–306*, 2524–2527. [CrossRef]
23. Lapovok, R.; Gao, X.; Nie, J.; Estrin, Y.; Mathaudhu, S.N. Enhancement of properties in cast Mg–Y–Zn rod processed by severe plastic deformation. *Mater. Sci. Eng. A* **2014**, *615*, 198–207. [CrossRef]
24. Kim, W.J.; Hong, S.I.; Kim, Y.S.; Min, S.H.; Jeong, H.T.; Lee, J.D. Texture development and its effect on mechanical properties of an AZ61 Mg alloy fabricated by equal channel angular pressing. *Acta Mater.* **2003**, *51*, 3293–3307. [CrossRef]

25. Stanford, N. Micro-alloying Mg with Y, Ce, Gd and La for texture modification—A comparative study. *Mater. Sci. Eng. A* **2010**, *527*, 2669–2677. [CrossRef]
26. Sauvage, X.; Wilde, G.; Divinski, S.V.; Horita, Z.; Valiev, R.Z. Grain boundaries in ultrafine grained materials processed by severe plastic deformation and related phenomena. *Mater. Sci. Eng. A* **2012**, *540*, 1–12. [CrossRef]
27. Bohlen, J.; Yi, S.B.; Swiostek, J.; Letzig, D.; Brokmeier, H.G.; Kainer, K.U. Microstructure and texture development during hydrostatic extrusion of magnesium alloy AZ31. *Scr. Mater.* **2005**, *53*, 259–264. [CrossRef]
28. Lentz, M.; Klaus, M.; Beyerlein, I.J.; Zecevic, M.; Reimers, W.; Knezevic, M. In situ X-ray diffraction and crystal plasticity modeling of the deformation behavior of extruded Mg–Li–(Al) alloys: An uncommon tension–compression asymmetry. *Acta Mater.* **2015**, *86*, 254–268. [CrossRef]
29. Li, Z.; Zhou, S.; Huang, N. Effects of ECAE processing temperature on the microstructure, mechanical properties, and corrosion behavior of pure Mg. *Int. J. Miner. Metall. Mater.* **2015**, *22*, 639–647. [CrossRef]
30. Humphreys, F.J.; Hatherly, M. *Recrystallization and Related Annealing Phenomena*, 2nd ed.; Elsevier: Amsterdam, The Netherlands, 2004; pp. 219–224.